IEEE Access
Multidisciplinary | Rapid Review | Open Access Journal

Received October 23, 2019, accepted December 6, 2019, date of publication December 13, 2019,
date of current version December 23, 2019.

Digital Object Identifier 10.1109/ACCESS.2019.2958956

Unraveling the "U-Shaped" Dependence of Surface Flashover Performance on the Surface Trap Level

SHENGTAO LI, (Senior Member, IEEE), ZHEN LI, YIN HUANG, HAOMING XU, FAROOQ ASLAM, DAOMIN MIN, AND WEIWANG WANG

State Key Laboratory of Electrical Insulation and Power Equipment, Xi'an Jiaotong University, Xi'an 710049, China

Corresponding author: Shengtao Li (sli@mail.xjtu.edu.cn)

This work was supported in part by the National Key Research and Development Program of China under Grant 2017YFB0902702, in part by the National Natural Science Foundation of China (NSFC) under Grant 51337008, in part by the Science and Technology Project of State Grid, China, under Grant 52110418000R, in part by the Foundation Project of State Grid in Shaanxi Province Section, China, under Grant SGSNKY00SPJS1900302, and in part by the Key Research and Development Program of Shaanxi Province under Grant 2018ZDCXL-GY-07-04.

ABSTRACT The effects of surface traps on surface flashover remain controversial. To clarify the relation between surface flashover and surface trap level, in this work, the surface trap level of epoxy composites was modified by nanoparticles incorporation, electron beam irradiation, and ozone treatment. Surface trap characteristics were analyzed by surface potential decay. Surface flashover voltages were measured in a vacuum for dc voltage and in SF_6 for ac voltage. The "U-shaped" curve is founded to describe the relation between surface flashover voltage and surface deep trap level, surface flashover voltage first decreases and then increases with surface deep trap level. Enhancement of surface flashover voltage is attributed to reduced surface charge density, which was calculated by a double-trap flashover model. The simulation results indicate that the surface charge density on left side of "U-shaped" curve is controlled by surface shallow traps, whereas that on the right side is determined by surface deep traps. The effects of surface shallow and deep traps on surface charge accumulation and dissipation are used to demonstrate the reduced surface charges and improved surface flashover voltage for the "U-shaped" curve. The proposed "U-shaped" curve offers a promising way to improve surface flashover performance for high-voltage applications by tailoring surface trap characteristics with surface modifications.

INDEX TERMS Surface flashover, surface trap level, surface charge, epoxy composites.

I. INTRODUCTION

Epoxy resins (EP) with excellent mechanical and electrical performance are used extensively in advanced spacecraft and extra-high voltage power applications [1]–[5]. However, surface flashover is an intractable problem for that epoxy-based equipment because the surface flashover voltage is lower than the breakdown voltage with the same gap distance [6]. Therefore, it's important to improve surface flashover performance for epoxy resin. There are several factors influence surface flashover, such as voltage waveforms, gas species, materials, surface charge, and the shape of insulators and electrodes, etc. [7]–[9]. In particular, surface charge characteristics are closely linked to surface flashover and have been increasingly studied in recent research [10]–[14]. It is widely acknowledged that charges accumulating on a solid surface distort the local electric field and increase the probability of surface flashover performances [15]. Hence, surface modifications are necessary to reduce surface charges and improve the surface flashover performance of EP.

Several physical and chemical surface modifications can be used for polymer dielectrics, such as heat treatment, electron beam irradiation, plasma treatment, fluorination treatment, ozone treatment, surface coating, and nanoparticles incorporation. [16]–[19]. Notably, surface trap characteristics, which are crucial factors for surface charges and surface flashover, are also changed by these surface modification methods [16], [17], [20]–[22]. Therefore, many studies have

The associate editor coordinating the review of this manuscript and approving it for publication was Jenny Mahoney.

investigated the effects of surface traps on surface flashover by surface modifications. Yu *et al.* [20] incorporated nano-TiO_2 into EP and investigated the relation between surface flashover voltage and surface trap level. A higher surface trap level suppressed the electron emission processes and improved surface flashover voltage, this effect was supported in [16], [23], [24]. Shao [17] *et al.* treated EP using plasma and founded surface flashover voltage decreases with surface trap level. A reduced surface trap level accelerated surface charge dissipation and improved surface flashover voltage, which was supported in [15], [17], [18], [21], [22]. These studies show that surface flashover voltage has an inverse relation to surface trap level. To date, the effects of surface traps on surface flashover remain controversial.

To address the controversial relationship between surface flashover and surface trap, In this work, epoxy composites are surface-modified by nanoparticles incorporation, electron beam irradiation and ozone (O_3) treatment, surface trap characteristics were analyzed by surface potential decay curves, dc and ac surface flashover voltages were measured in a vacuum and in SF_6 respectively, Surface charge density and electric field distributions were calculated by a double traps flashover model. ''U-shaped'' curves for the relationship between surface flashover voltage and surface trap level were established in various gas species and voltage forms, and effects of surface traps on surface flashover were investigated.

II. METHODS

A. SAMPLE PREPARATION

Liquid state bisphenol-A E-51 EP ($\rho = 1.03$ g/cm^3) was used. The curing agent was tetrahydromethylphthalic anhydride (type GH-9303, $\rho = 1.21$ g/cm^3), nano-titania [TiO_2, 10-30 nm diameter, treated by KH560, (2,3-epoxypropoxy) propytri-methoxysilane] and micro-alumina (Al_2O_3, 1 μm diameter) were selected as fillers, the accelerating agent for epoxy was tris(dimethylaminomethyl)phenol (DMP-30).

The procedures for preparing epoxy microcomposites and nanocomposites were as follows: particles were heated at 80°C for 12 h before sample preparation, and were grinded (only for nanoparticles) and added into the curing agent. An IKA T25 high-speed shearing machine was used to disperse nanoparticles for 15 min at 5200 r/min. For both nanocomposites and microcomposites, the turbid liquid was stirred 2000 r/min and defoamed 2200 r/min both for 10 min using a THINKY blender. To disperse particles, An ICQ-100KDE ultrasonic equipment with a power level of 99 W was used for 10 min. Then accelerating agent and epoxy resin were added into the turbid liquid and the processes of stirring, defoaming, and ultrasonic treatment were repeated. The epoxy composites were cured at 80°C for 4 h and then at 120°C for 8 h.

The filler contents of four epoxy nanocomposites were 0.5 wt%, 1 wt%, 2 wt%, 5 wt% (named x wt%, x is weight percentage of nano-TiO_2), and that of epoxy microcomposites was 60 wt% (named Micro). The samples were cleaned by ethanol for 10 min with ultrasonic equipment, and then dried at 60°C for 12 h.

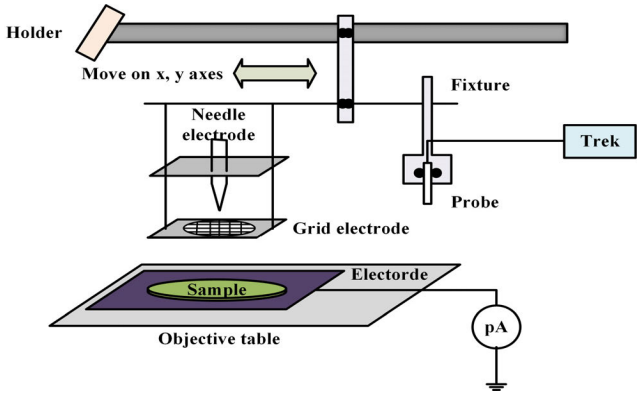

FIGURE 1. Scheme of surface potential decay system.

B. SURFACE MODIFICATION

Epoxy microcomposites samples were placed onto the constructed platform in a vacuum chamber. The bottom sides of the samples were connected with the ground. An electron gun was located approximately 400 mm above the platform. The gas pressure was lower than 5×10^{-4} Pa. The beam current was set to 5 μA and then the aluminum plate for electronic gun was removed. The electron beam energy were 5 keV, 10 keV, and 20 keV (named x keV, x is electron beam energy) respectively. Irradiation was maintained for 5 min.

Epoxy microcomposites samples treated by ozone were hanged on the metal holders in the chamber, a CF-G40 ozone treatment machine was used to generate O_3 into chamber. The gas pressure of the chamber was 0.14 MPa and the O_3 concentration was 140 mg/L. The samples were treated for 0.5 h, 1 h, 2 h, and 4 h (named x h, x is O_3 treatment time) as the gas pressure was maintained.

C. SURFACE POTENTIAL DECAY

The isothermal surface potential decay (SPD) system comprises aa dc charging unit, a surface potential recording unit and a temperature control unit. The whole SPD system was first stablized at 30°C. Then the sample surfaces were charged for 2 min with -10 kV for the grid electrode and -6 kV for the needle electrode. Then, the specimens were moved down to the noncontracted type surface potential electrostatic voltmeter (Trek0809). The surface potential was recorded, and the surface potential at a sample interval was 1 s. The samples were 1.5 mm. The scheme of SPD equipment is shown in Fig. 1.

D. SURFACE FLASHOVER MEASUREMENT

Surface flashover voltage was tested using a high voltage measurement chamber. The chamber was evacuated by a mechanical pump and a molecular pump to a gas pressure of 3×10^{-3} Pa for surface flashover test in vacuum. SF_6 gas was injected to 0.2 MPa for surface flashover test in SF_6.

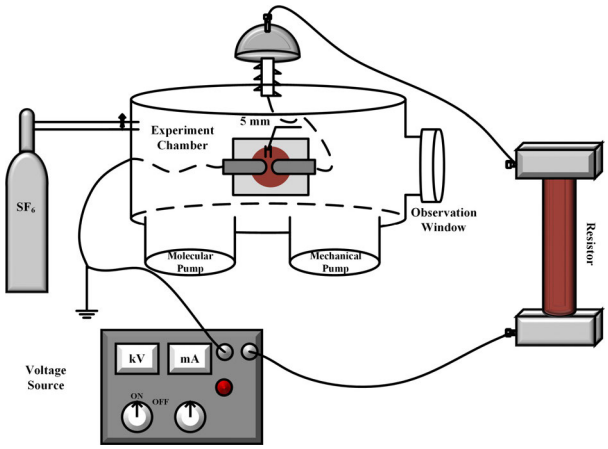

FIGURE 2. Scheme of surface flashover system (DC).

The chamber was kept stable for 10 min before thesurface flashover test.

Stainless steel finger type electrodes with a 5 mm gap distance and a 20 mm tip diameter were used to test the surface flashover. The ac voltage raised with 1 kV/s, and a step-raising method was used to test dc surface flashover voltage with 2 kV at each step. The voltage was stable for 30 s at each step. Six measurements were done for each specimen and three specimens were tested for each kind of epoxy composite. The surface flashover voltage was recorded as four or continuous discharges were observed. The surface flashover voltage was the averaged flashover values. The scheme of the flashover measurement system is shown in Fig. 2.

E. CALCULATION OF SURFACE FLASHOVER VOLTAGE

A Matlab®Program was used to calculate surface flashover voltage, surface charge density and electric field distribution. In that program, we compared the effects of deep and shallow surface traps on the charge transport process. The double-trap flashover calculation program is comprised of 6 steps [6], [25], [26]: 1) Set initial physical parameters. Input sample thickness, permittivity, voltage rise rate. 2) Grid discretization. Divided the discharging gap into 500 equal parts above and below the solid surface. The interval calculation time is 0.005 s 3) Initialized grid parameters. Set charge density, electric field and current density to zero. 4) Select a representative surface trap, we use the surface trap which has a higher value of P_{tr}/P_{de} (P_{tr} and P_{de} are the probabilities for carrier trapping and detrapping). 5) considering surface charges transport process. Calculate current density, electric field and surface charge density by the Poisson's equation, the continuity equation of the electrical current, the charge transport equation, the spatial integration of electric field equation, the injected current, and the trapping and detrapping dynamics equation. 6) Calculate flashover voltage. Set a critical current value for triggering flashover, as the current is higher than the critical value, stop the program and record the applied flashover voltage.

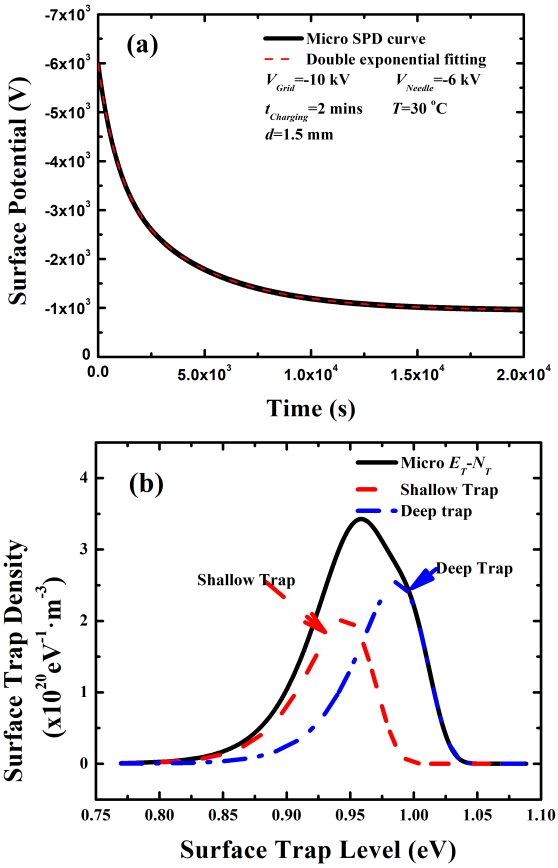

FIGURE 3. Surface potential decay system and result of Micro (a) SPD curve; (b) Surface trap level and density distribution).

III. RESULTS

A. SURFACE TRAP CHARACTERISTICS

Fig. 3 shows the SPD curve and surface trap characteristics of the Micro samples. Fig. 3a shows SPD curve exponentially decay over time. Surface trap characteristics are calculated by SPD curve in Fig. 3b. Two peaks of the curve are surface shallow and deep traps Horizontal and vertical coordinates of the maximum points are regarded as the surface trap characteristics, that is. surface trap level and density. All SPD results are elaborated in the Appendix A. The detailed processes of the surface trap characteristics calculated by SPD curves are elaborated in the Appendix B.

Fig. 4a shows the surface trap characteristics of the epoxy nanocomposites. In Fig. 4a, for 0 wt% samples, the surface shallow and deep trap level is 0.995 eV and 1.039 eV respectively. As filler contents increase, the surface deep trap level increases to 1.082 eV for 2 wt% sample. As filler loadings further increase, surface deep trap level and density decreases rapidly. Surface trap characteristics can be tailored by the interfacial properties of the nanoparticle matrix by introducing various filler contents of nanoparticles into the epoxy. Nanoparticles connect with molecular chains by ionic bonds, covalent bonds, hydrogen bonds, and some other strong interaction forces. Electrostatic barriers are established at the interface region, and some unsaturated functional

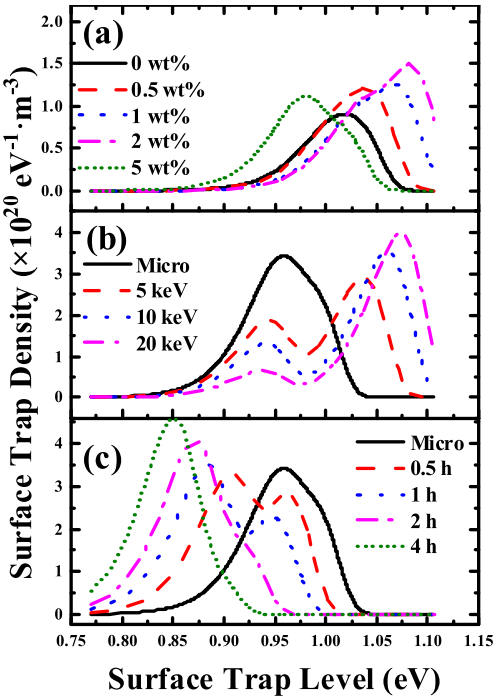

FIGURE 4. Surface trap characteristics of epoxy composites of (a) nanocomposites, (b) microcomposites irradiated by electron beam, and (c) microcomposites treated by O_3.

groups on the nanoparticle surfaces capture the electrons to maintain electrostatic balance [27], [28]. As filler contents first increase, carriers are captured by the unsaturated bonds at the interfacial region, which suppresses charge transport on the solid surface, surface deep trap level and density increase. As filler contents further increase, the distances between nanoparticles decrease and the interfacial region gradually overlaps. The interaction between nanoparticles and the matrix are weakened, thus surface deep trap level and density decrease.

Fig. 4b shows the surface trap characteristics for the epoxy microcomposites irradiated by the electron beam. Because many traps are introduced by microparticles, the trap characteristics of the Micro samples are different from 0wt%. Fig. 4b shows that the surface deep trap level increases with irradiation beam energy. the sample with an electron beam energy of 20 keV and a surface deep trap level of 1.072 eV improved compare with the Micro sample of 0.997 eV, whereas the surface shallow trap level barely changed. Simultaneously, the surface shallow trap density decreases and the deep trap density increases with the electron beam energy. An electron beam with high energy breaks the side and terminal groups of epoxy molecular chains, and many free radicals and terminal groups are generated [16], [29]. Free radicals and terminal groups have strong abilities to capture the carriers; as a result, some shallow traps are converted to deep traps by electron beam irradiation. As the electron beam energy increases, the capacity for bond breaks increases, and thus the surface deep trap level and density further increase.

Fig. 4c shows the surface trap characteristics of the epoxy microcomposites treated by O_3. As treatment time increases, the surface trap level clearly decreases, the surface deep trap density decreases and shallow trap density increases. The O_3 reacts with hydroxyl and generates carbonyl in epoxy molecular chains [21], [30]. The polarity of "C = O" bonds is lower than that of "-OH" bonds, which indicate that the carriers were not easily captured by the O_3 treatment, and surface deep traps are converted to shallow traps [30]. As treatment time increases, many hydroxyl groups are generated, the surface deep trap density decreases and the shallow trap density increases.

B. SURFACE FLASHOVER PERFORMANCES

Fig. 5a shows surface flashover voltages of epoxy nanocomposites in a vacuum with dc voltage and in SF_6 with ac voltage. The surface flashover voltage of 0 wt% samples are 33.07 kV and 22.56 kV in a vacuum and in SF_6 respectively. As filler contents increase, the surface flashover voltage increases up to 2 wt%. The surface flashover voltage of 2 wt% samples are 37.85 kV and 26.61 kV, which improve 14.45% and 16.62% compare with those of pristine EP in the vacuum and in SF_6. As filler contents further increase, the surface flashover voltage decreases both in the vacuum and in the SF_6. For 5 wt% samples, the surface flashover voltage decreases 8.01% and 4.43% compare with those of 0 wt% samples.

Fig.5b and 5c show the surface flashover voltages of EP-Al_2O_3 microcomposites treated by the electron beam and the O_3. The surface flashover voltage of Micro samples are 34.21 kV and 23.27 kV in a vacuum and in SF_6. In Fig. 5b, surface flashover increases with electron beam energy, the surface flashover voltage of 20 keV samples improve 8.80% and 11.13% in the vacuum and in SF_6 compare with those of Micro samples. In Fig. 5c, surface flashover voltage increases with the duration of the O_3 treatment. Surface flashover voltage of 4 h samples increase 11.27% and 25.27% compare with those of Micro samples.

IV. DISCUSSION

A. "U-SHAPED" CURVE

Fig. 6 shows the relation between the surface flashover voltage and surface deep trap level in a vacuum (Fig. 6a) and in SF_6 (Fig. 6b) for epoxy composites. In Fig. 6, the surface flashover voltage firstly decreases and finally increases with the surface deep trap level. The curves are "U-shaped"; Ozone treatment samples are on the left side of the curve, and nanocomposites and electron beam irradiation samples are on the right side. The surface deep trap levels corresponding to the lowest points of the "U-shaped" curves are 1.010 eV and 1.016 eV in the vacuum and in SF_6 respectively.

B. EFFECTS OF SURFACE TRAPS ON SURFACE FLASHOVER PERFORMANCES

Surface flashover occurring on a solid surface comprises several physical processes: initial electron emission: initial

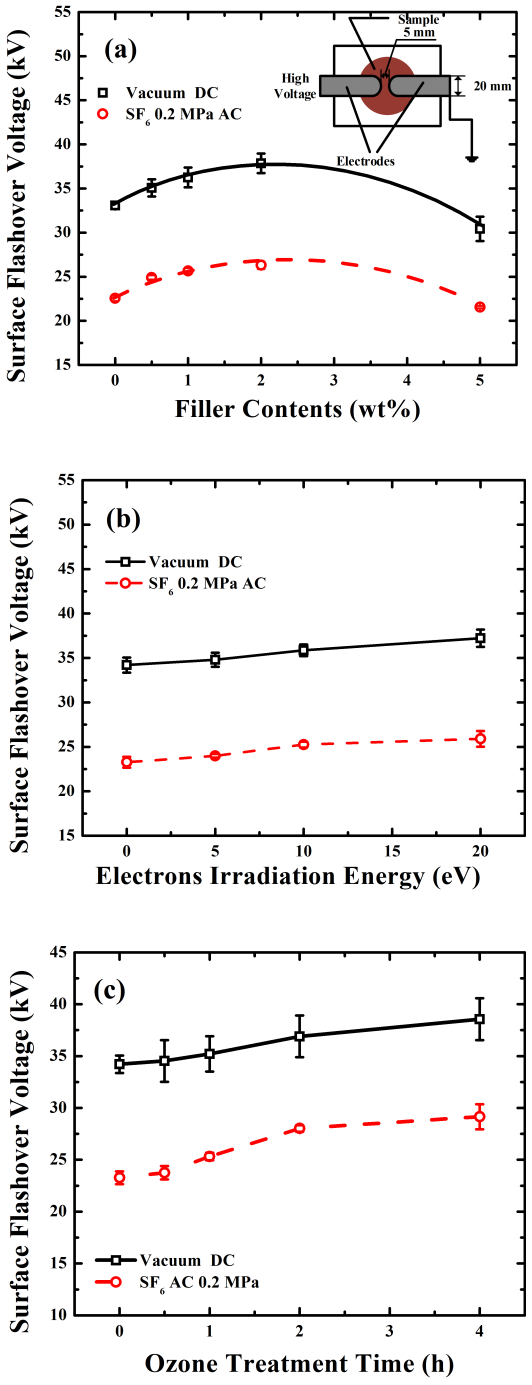

FIGURE 5. Surface flashover characteristics of epoxy composites of (a) nanocomposites, (b) microcomposites irradiated by an electron beam, and (c) microcomposites treated by O_3. Lines in (a) are trend lines for the surface flashover results.

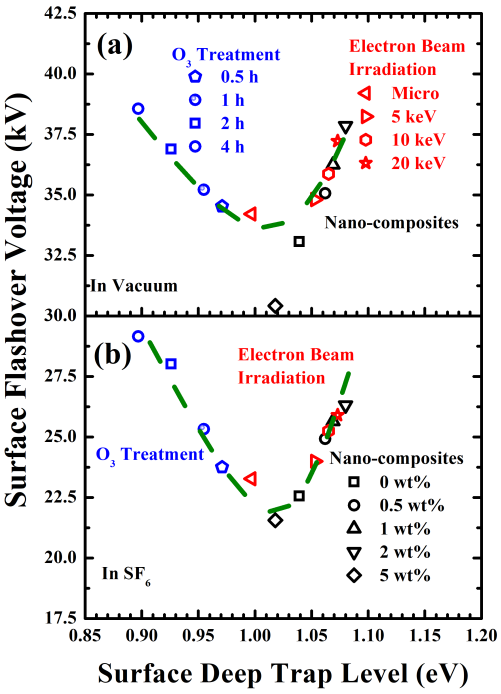

FIGURE 6. Relation between surface flashover voltage and surface deep trap level, i.e., "U-shaped" curves of epoxy nanocomposites in a (a) vacuum and in (b) SF_6. The red dashed line is the trend line.

electrons bump onto the solid surface; secondary electron emission; secondary electron avalanche; gas adsorption-/desorption; gas molecule collision ionization; plasma migration; and surface flashover path formation [3], [7]–[9], [31], [32]. Initial electrons are emitted from triple junction points by an applied external field, and some positive space charges are trapped on the solid surface. Surface positive charges attract the charges transported on solid surface; as a result, accelerated electrons strike the solid surface and excite the trapped secondary electrons. These secondary electrons constantly acquire energy from the electrical field and restrike the solid surface to generate more secondary electrons, which causes an electron avalanche and a further accumulation of positive charges on the solid surface. On the other hand, the secondary electrons collide with the gas molecules in the adsorption/desorption layer to cause impact ionization, finally forming a fast and highly conductive plasma near the anode. Surface flashover path is formed as the plasma extends to anode electrode.

Surface flashover is strongly related to surface charge density. Generally, accumulated positive charges distort the electric field on the solid surface, which reduces surface flashover performance. Therefore, it is important to investigate the effects of surface traps on surface charge density. Surface trap characteristics influence mainly trapping and detrapping processes for carriers. The trapping and detrapping probability are described in [33]:

$$P_{tr} = eN_t\mu_0/4\varepsilon_0\varepsilon_r \quad (1)$$

$$P_{de} = \upsilon_{ATE}\exp\left(-E_t/k_BT\right) \quad (2)$$

where, μ_0 is carrier mobility in $m^2/V{\cdot}s$ (the value of μ_0 is calculated by SPD curve, which is described in Appendix C), υ_{ATE} is attempted escape frequency in s^{-1}, E_t is surface trap level in eV, $N_t(E_t)$ is surface trap density in $eV^{-1}{\cdot}m^{-3}$. ε_0 is permittivity in vacuum (8.854×10^{-12} F/m), ε_r is the relative permittivity. k_B is Boltzmann constant (1.382×10^{-23} J/K). T is temperature in K. e is charge quantity (1.602×10^{-19} C).

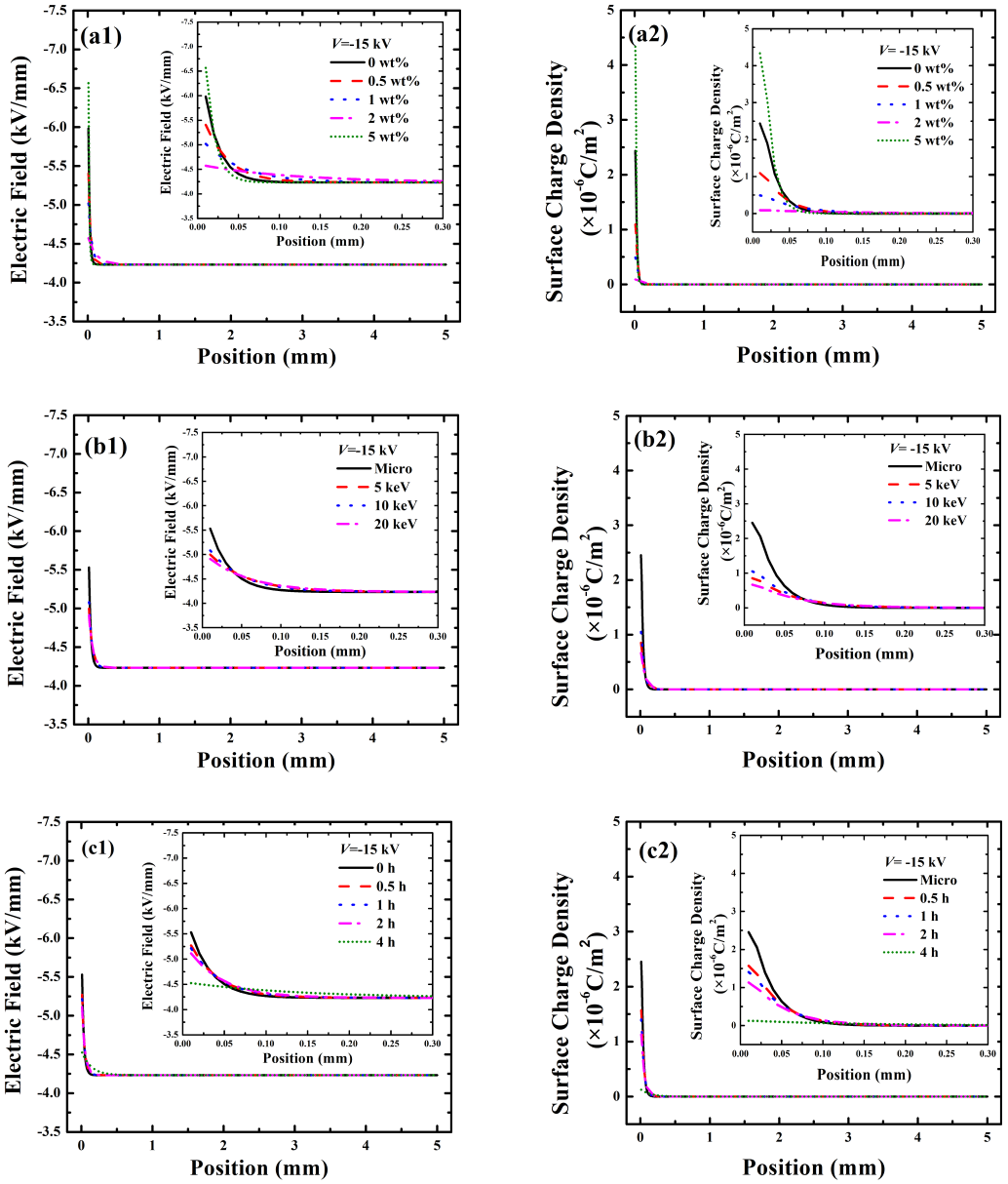

FIGURE 7. Electric field and surface charge density distributions of epoxy composites of (a1, a2) nanocomposites, (b1, b2) microcomposites irradiated by electron beam, and (c1, c2) microcomposites treated by O_3. The externally applied voltage was -15 kV.

The value of P_{tr}/P_{de} determines the importance of surface traps in charge transport process [33], [34]. In the double-trap flashover model, we use the surface trap characteristics that have the larger P_{tr}/P_{de} value to calculate surface charge density and electric field distribution. The surface shallow trap is the representative trap for the ozone treatment samples, whereas the surface deep trap is preferred for nanocomposites and electron beam irradiation samples.

Fig. 7 shows surface charge densities and electric field distributions of epoxy composites when the applied voltage is -15 kV. Electric fields are severely distorted near the cathode and large amounts of positive charges are accumulated in this area. For the nanocomposites in Fig. 7a, the surface charge density and the electric field near the cathode firstly decreases and finally increases with filler contents. For the microcomposites irradiated by electron beam in Fig. 7b, the surface charge density and the electric field near the cathode decreases with irradiation energy. For the microcomposites treated by O_3 in Fig. 7c, the surface charge density and electric field decreases with ozone treatment duration. From Fig. 5 and 7, the accumulated positive charges distort local electric field and decrease surface flashover voltage, which is appropriate for both sides of the "U-shaped" curve. However, the effects of surface traps on the surface flashover performances at the two sides of the curve are different.

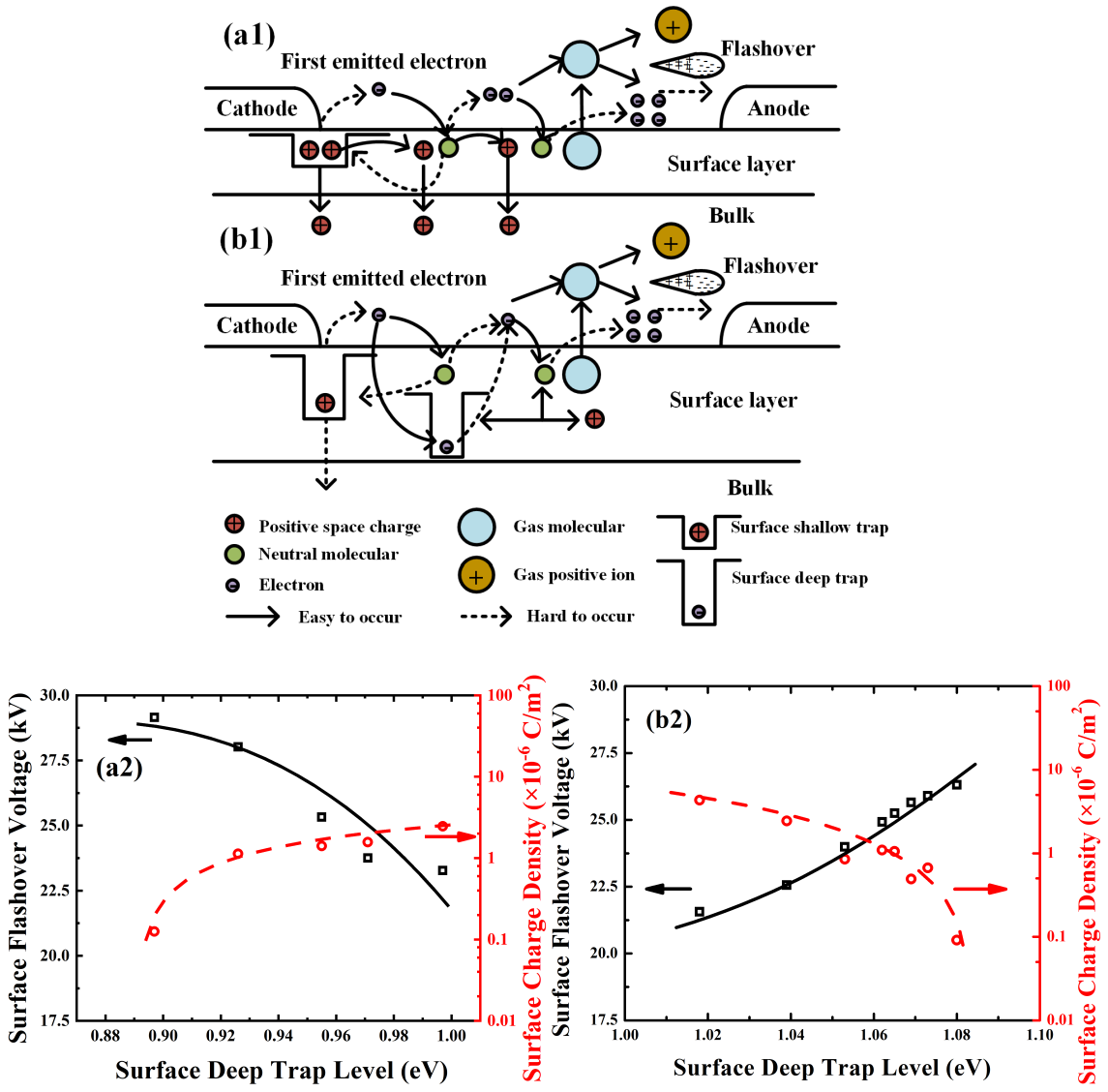

FIGURE 8. Effects of surface (a1) shallow and (b1) deep traps on surface flashover performances. (a2) shows surface flashover voltage and surface charge density on the left part of "U-shaped" curve, (b2) shows surface flashover voltage and surface charge density on the right part of "U-shaped" curve.

Fig. 8 shows the synthetic effects of surface deep and shallow traps on surface flashover performances. For the left part of the "U-shaped" curve in Fig. 8a1, the electrons are emitted by a distorted electric field at triple junction point, and left behind lots of positive charges near the cathode. Since surface conductivity and mobility are high in this case, the surface charges near the cathode are likely to dissipate to the bulk and the surface. Electrons in the gas are accelerated by the electric field. Because some positive charges accumulate on the dielectric surface, electrons are attracted and strike the solid surface; Some of electrons stimulated the secondary electrons, and some positive charges are generated on the dielectric surface, the surface charges probably dissipate along the surface or into the bulk as well. Secondary electrons acquire energy from the electric field and re-strike the surface to generate lots of secondary electrons. Those electrons collide with gas molecules and cause impact ionization. Lots of positive ions generated by impact ionization and secondary electrons form plasma. The surface flashover is triggered as the plasma extends to the anode. In these physical processes, as the deep trap level increases, surface conductivity and carrier mobility are reduced by the increase of surface shallow trap level and the decrease of shallow trap density. The trapped positive charges on the solid surface are hard to dissipate along the surface and into the bulk. The surface electrical field is severely distorted by the accumulated positive charges, so the surface flashover voltage decreases, which is shown in Fig. 8a2. In this case, surface flashover characteristics of epoxy composites are dominated by shallow trap level and density, and surface flashover voltage decreases

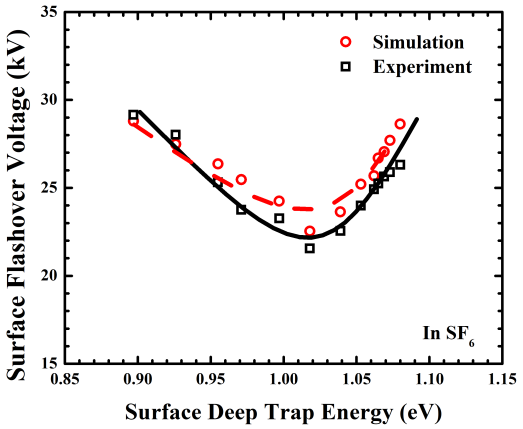

FIGURE 9. Experimental (black points and line) and calculated (red points and line) "U-shaped" curves.

with the increase of deep trap level on the left side of "U-shaped" curve.

For the right side of "U-shaped" curve in Fig. 8b1, the flashover physical processes are similar to that on the left part of "U-shaped" curve, but there are still some differences. In this case, surface conductivity and mobility are low, and surface and bulk dissipation are not crucial influence factors for surface flashover. As surface deep trap level increases, the electrons are hardly to be emitted from the cathode and solid surface, and initial and secondary electron emission processes are suppressed. The neutral molecules not easily ionized by injected electrons and the amount of surface positive charges are reduced. The local electric field on the solid surface becomes uniform, and surface flashover voltage increases in Fig. 8b2. On the right part of "U-shaped" curve, surface flashover characteristics are determined by deep trap, and the behaviors of surface deep traps in surface flashover development indicates that surface flashover voltage increases with deep trap level.

Fig. 9 shows the experimental and calculated surface flashover voltages of epoxy composites in SF_6 with 0.2 MPa gas pressure. The minimum value of surface deep trap level for the lowest surface flashover voltage is 1.015 eV. The surface flashover voltage is enhanced 25.27% and 22.25% for the experimental and simulation results, respectively. Both flashover voltages decrease and then increase with surface deep trap level. The simulation results closely agree with the experimental results. And the "U-shaped" curve is further verified by surface flashover simulation.

Finally, the different mechanisms of ac flashover and dc flashover need to be discussed. Ac flashover voltage is always less than the dc flashover voltage [37], [38]. As mentioned previously, surface charge characteristics plays an important role in surface flashover. For ac surface flashover, the applied voltage changes very quickly, and the carriers captured in traps do not have enough time to escape from the traps. Therefore, the surface charge density of samples under an ac supply is higher than that under a dc supply with the same applied voltage, the electric field distorts and flashover voltage decreases, which is supported in [39]. Surface traps play the same roles in ac and dc flashover physical process, i.e. capture the carriers and accumulate surface charge. However, the difference between dc and ac flashover voltages is account for the time taken by carriers to escape from the traps.

V. CONCLUSION

In this work, the surface trap level of epoxy composites were surface-modified by nanoparticles incorporation, electron beam irradiation, and ozone treatment. The relationship between surface flashover and surface trap was established, and synthetic effects of surface traps on surface flashover were studied. On the basis of experimental and simulation results, main conclusions are summarized as follows:

1) a "U-shaped" relation is established between surface flashover voltages and surface deep trap levels. The nanoparticles incorporation and electron beam irradiation samples are on the right side of "U-shaped" curves, while ozone treatment samples are on the left side. The surface deep trap levels of the lowest points of "U-shaped" curves are 1.010 eV and 1.016 eV in a vacuum and in SF_6, respectively.

2) The reduced surface shallow trap level accelerates surface charge dissipation, while the increased surface deep trap level suppresses electron emission processes. Both surface trap behaviors reduce surface charge density and improve surface flashover performance, resulting in the "U-shaped" curves.

3) The discovery of the "U-shaped" curve reveals the synthetic effects of surface traps on surface flashover, while previous studies focused on one side of the curve. The "U-shaped" curves are appropriate for various gas species and voltage forms, and thus offer a promising route for improve surface flashover performance for high-voltage applications by tailoring surface trap characteristics with surface modifications.

APPENDIX

A. SPD RESULTS

Fig. 10 shows SPD results of epoxy composites.

B. SURFACE TRAP ANALYSIS

Fig. 3a describes a surface potential decay process for the Micro samples. Double exponential function was employed to fitting the SPD curve, and surface trap characteristics were analyzed by Simmon's theory. Generally, the charge density on a single trap level follows Femi-Dirac distribution. The double exponential function, and surface trap level and density were calculated in the following equation [6], [35]:

$$\phi(t) = y_0 + A_1 \exp\left(-\frac{t}{x_1}\right) + A_2 \exp\left(-\frac{t}{x_2}\right) \quad (3)$$

$$E_t = k_B \ln(\nu_{ATE} t) \quad (4)$$

$$N_t(E_t) = \frac{\varepsilon_0 \varepsilon_r}{elL} t \frac{dV_s(t)}{dt} \quad (5)$$

In (3-5), $\Phi(t)$ is surface potential at time t. A_1, A_2, x_1, x_2 are parameters which related to surface trap density and level. L

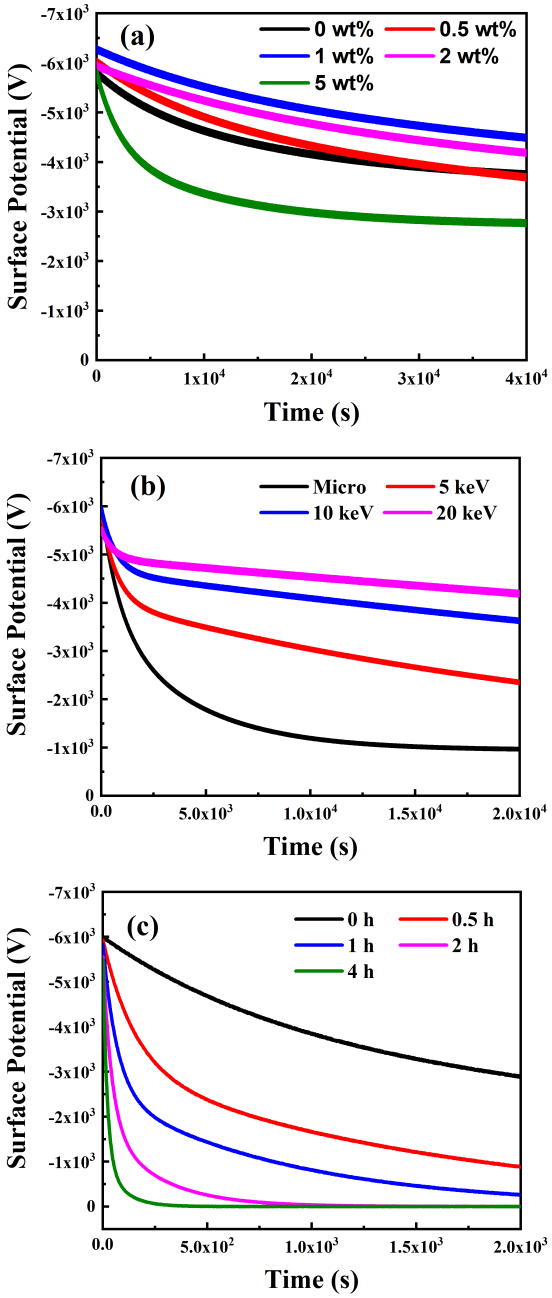

FIGURE 10. Surface potential decay results of epoxy composites of (a) nanocomposites, (b) microcomposites irradiated by electron beam, and (c) microcomposites treated by O_3.

is sample thickness in m (1.5×10^{-3} m), l is injected charge depth which is assumed to be 1 μm, $V_s(t)$ is surface potential at t in V. From (4) and (5), surface trap energy and density were calculated in Fig. 3b.

C. MOBILITY ANALYSIS

Carrier mobility controlled by surface trap characteristics can be calculated by SPD curves. The mobility μ is described as [36]:

$$-\frac{d\phi\,(t_0)}{dt} = \frac{\mu}{2}\left(\frac{\phi\,(t_0)}{l}\right)^2 \tag{6}$$

where, $\Phi(t_0)$ is the primary SPD surface potential in V. The left part of (6) is controlled by both surface deep and surface shallow traps in (3), so the carrier mobility of deep and shallow traps can be calculated by (6).

Fig. 11 shows the carrier mobility of surface deep and shallow traps for the ozone treatment samples. As shown in Fig. 11, the carrier mobility increases with ozone treatment duration, which indicates that conductivity increases with ozone treatment duration. Besides, the mobility of surface shallow traps is much higher than that of surface deep traps on the left side of the "U-shaped" curve.

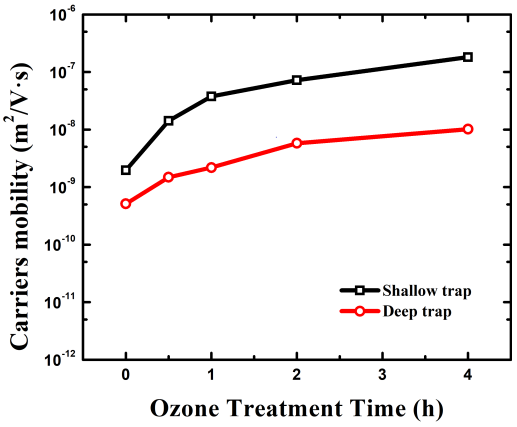

FIGURE 11. Carrier mobility controlled by surface shallow (black line) and deep trap (red line).

D. SURFACE CONDUCTIVITY

Surface conductivity of epoxy composites was conducted by a Keithley 6517 electrometer with a three-electrode structure and a 8009 resistance box. The conductivity was tested 8 times for each epoxy composite at 800 V. The surface conductivity was the averaged results, and the peak-to-peak values of the results is less than 20%.

The results show that the surface conductivity of the epoxy composites varied little with either nanoparticle incorporation aor electron beam irradiation, which indicate that surface dissipation process is not a crucial factor for surface flashover on the right part of the "U-shaped" curve. However, surface conductivity increases with ozone treatment time in Fig. 12a, the surface conductivity of 4 h samples is about 84 times that of Micro samples. Hence, surface dissipation is a crucial factor on the left of the "U-shaped" curve. The relation between surface flashover voltage and surface conductivity of epoxy composites treated by O_3 is shown in Fig. 12b.

E. SURFACE FLASHOVER MODEL

Fig. 13 is the surface flashover calculation model in our test. The surface flashover model is divided into the charge transport process in solid and gas. The model comprises many physical processes:

1) Applied voltage:

DC and AC applied voltage:

$$V = V_{appl} \times t \tag{7}$$

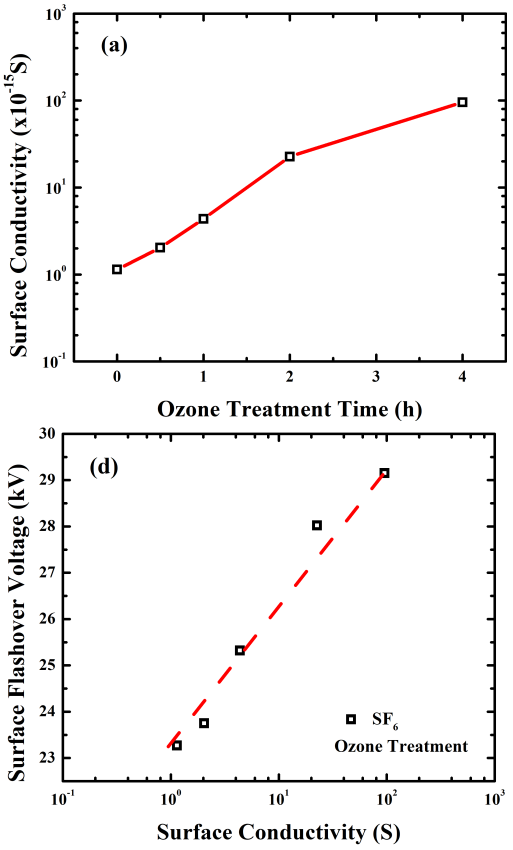

FIGURE 12. (a) Surface conductivity of epoxy microcomposites treated by O_3, and (b) relation between surface flashover voltage and surface conductivity.

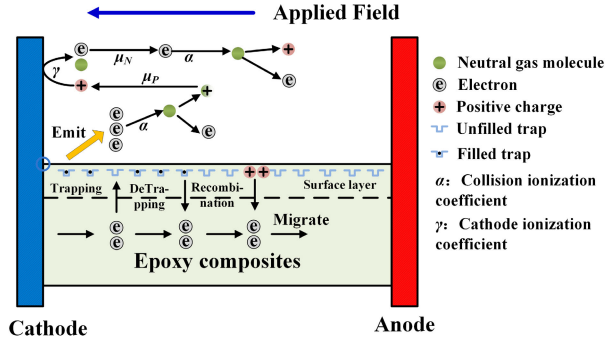

FIGURE 13. Surface flashover calculation model of epoxy composites.

$$V = V_{appl} \times t \times \sin(2\pi ft) \tag{8}$$

where, V_{appl} is voltage raise rate, t is the time, f is the AC frequency.

2) Charge injection:

The current injection equation:

$$j_{CTJ(e)}(t) = AT^2 \exp\left(-\frac{E_{in(e)}}{k_B T}\right) \exp\left(\frac{\sqrt{e^3 F(0,t)/4\pi\varepsilon_0\varepsilon_r}}{k_B T}\right) \tag{9}$$

where, $j_{CTJ(e)}(t)$ is the current density of inject electrons; A is Richard constant; T *is* temperature; $E_{in(e)}$ is the contact barrier; e is the electron charge; ε_0 is permittivity in vacuum. ε_r is relative permittivity.

3) Electron conduction:

$$j_{sc(e)}(x,t) = en_{sf(e)}(x,t)\,\mu_{s0(e)}F(x,t) \tag{10}$$

where, $j_{sc(e)}(x,t)$ is surface current density; $n_{sf(e)}(x,t)$ is the free charge density; $\mu_{s0(e)}$ is the mobility for electron; $F(x,t)$ is electric field.

4) Trapping and detrapping coefficient:

In the manuscript, the equation (1) and (2) are trapping and detrapping coefficient.

5) Trap selection:

Calculate the P_{de}/P_{tr} of deep and shallow trap, the trap level and density of the trap with higher P_{de}/P_{tr} value are used to calculate the trapping and detrapping dynamical equation.

6) Trapping dynamical equation:

$$\frac{dn_{sf(e)}(x,t)}{dt} = -P_{str(e)}n_{sf(e)}(x,t)\left[1 - \frac{n_{sf(e)}(x,t)}{N_{st(e)}}\right] \tag{11}$$

where, $P_{str(e)}$ is the probability for electron capture; $N_{st(e)}$ is the trap density.

7) Detrapping dynamical equation:

$$\frac{dn_{st(e)}(x,t)}{dt} = -P_{sde(e)}n_{st(e)}(x,t) \tag{12}$$

where, $P_{sde(e)}$ is the electron detrapping probability; $n_{st(e)}$ is the density of trapped electrons.

8) Charge density in dielectric:

$$Q_{total}(x,t) = -en_{sf(e)}(x,t) - en_{st(e)}(x,t) \tag{13}$$

where, $Q_{total}(x,t)$ is charge density in dielectric.

9) Poisson's equation:

$$\frac{\partial^2\varphi(x,t)}{\partial x^2} = -\frac{Q_{total}(x,t)}{\varepsilon_0\varepsilon_r} \tag{14}$$

where, ϕ is surface potential.

10) Gas molecular mean free path:

$$\lambda = \frac{1}{\pi r^2 N_g} = \frac{k_B T}{\pi r^2 P} \tag{15}$$

where, λ is mean free path; N_g is gas density, r is molecular radiu, P is gas pressure.

11) Collision ionization coefficient:

$$\alpha(x,t) = \frac{\pi r^2 P}{k_B T} \exp\left(-\frac{\pi r^2 P\phi_i}{k_B TE(x,t)}\right) \tag{16}$$

where, ϕ_i is the ionization potential for gas molecule.

12) Current density in Gas:

$$j(x,t) = j_0 \frac{e^{\int_0^x \alpha(x,t)dx}}{1 - \gamma\left(e^{\int_0^x \alpha(x,t)dx} - 1\right)} \tag{17}$$

where, γ is the cathode ionization coefficient.

13) Criterion:

$$j(x,t) \geq j_c \tag{18}$$

where j_c is the critical value for trigging surface flashover.

ACKNOWLEDGMENT

Authors thanks to Associate Prof. Le Zhang for detailed suggestions for this manuscript. Author Zhen Li thanks to Kaiyue Ma for her encouragement and help in this work.

REFERENCES

[1] S. Li, S. Pan, G. Li, D. Min, W. Wang, and S. Li, "Influence of electron beam irradiation on DC surface flashover of polyimide in vacuum," *IEEE Trans. Dielectr. Electr. Insul.*, vol. 24, no. 2, pp. 1288–1294, Apr. 2017.

[2] B. X. Du, R. R. Xu, J. Li, and Z. L. Li, "Improved carrier mobility dependent surface charge am flashover voltage of polypropylene film under DC and pulse voltages," *IEEE Trans. Dielectr. Electr. Insul.*, vol. 25, no. 3, pp. 1014–1021, Jun. 2018.

[3] F. A. M. Rizk and S. I. Kamel, "Modelling of HVDC wall bushing flashover in nonuniform rain," *IEEE Trans. Power Del.*, vol. 6, no. 4, pp. 1650–1662, Oct. 1991.

[4] B. X. Du, H. C. Liang, J. Li, and Z. Y. Ran, "Electrical field distribution along SG_6/N_2 filled DC-GIS/GIL epoxy spacer," *IEEE Trans. Dielectr. Electr. Insul.*, vol. 25, no. 4, pp. 1202–1210, Aug. 2018.

[5] P. Li, J. Fan, W. Li, Z. Su, and J. Zhou, "Flashover performance of HVDC iced insulator strings," *IEEE Trans. Dielectr. Electr. Insul.*, vol. 14, no. 6, pp. 1334–1338, Dec. 2007.

[6] S. Li, Y. Huang, D. Min, G. Qu, H. Niu, Z. Li, W. Wang, J. Li, and W. Liu, "Synergic effect of adsorbed gas and charging on surface flashover," *Sci. Rep.*, vol. 9, no. 1, p. 5464, Apr. 2019.

[7] H. C. Miller, "Surface flashover of insulators," *IEEE Trans. Electr. Insul.*, vol. 24, no. 5, pp. 765–786, Oct. 1989.

[8] H. C. Miller, "Flashover of insulators in vacuum: Review of the phenomena and techniques to improved holdoff voltage," *IEEE Trans. Electr. Insul.*, vol. 28, no. 4, pp. 512–527, Aug. 1993.

[9] H. C. Miller, "Flashover of insulators in vacuum: The last twenty year," *IEEE Trans. Dielectr. Electr. Insul.*, vol. 22, no. 6, pp. 3641–3657, Dec. 2015.

[10] B. Du, R. Chang, J. Jiang, and J. Li, "Temperature-dependent surface charge and flashover behaviors of oil-paper insulation under impulse with superimposed DC voltage," *IEEE Access*, vol. 6, pp. 63087–63093, 2018.

[11] Y. S. Liu, G. J. Zhang, W. B. Zhao, and Y. Zhang, "Analysis on surface charging of insulator prior to flashover in vacuum," *Appl. Surf. Sci.*, vol. 230, nos. 1–4, pp. 12–17, May 2004.

[12] B. X. Du and M. Xiao, "Influence of surface charge on DC flashover characteristics of epoxy/BN nanocomposites," *IEEE Trans. Dielectrics Electr. Insul.*, vol. 21, no. 2, pp. 529–536, Apr. 2014.

[13] C. Li, J. Hu, C. Lin, B. Zhang, G. Zhang, and J. He, "Surface charge migration and dc surface flashover of surface-modified epoxy-based insulators," *J. Phys. D, Appl. Phys.*, vol. 50, Apr. 2017, Art. no. 065301.

[14] B. Du and Z. L. Li, "Hydrophobicity, surface charge and DC flashover characteristics of direct-fluorinated RTV silicone rubber," *IEEE Trans. Dielectr. Electr. Insul.*, vol. 22, no. 2, pp. 930–940, Apr. 2015.

[15] C. Li, J. Hu, C. Lin, and J. He, "The control mechanism of surface traps on surface charge behavior in alumina-filled epoxy composites," *J. Phys. D, Appl. Phys.*, vol. 49, no. 1, Sep. 2016, Art. no. 445304.

[16] Y. Huang, D. Min, S. Li, Z. Li, D. Xie, X. Wang, and S. Lin, "Surface flashover performance of epoxy resin microcomposites improved by electron beam irradiation," *Appl. Surf. Sci.*, vol. 406, pp. 39–45, Jun. 2017.

[17] T. Shao, F. Liu, B. Hai, Y. Ma, R. Wang, and C. Ren, "Surface modification of epoxy using an atmospheric pressure dielectric barrier discharge to accelerate surface charge dissipation," *IEEE Trans. Dielectr. Electr. Insul.*, vol. 24, no. 3, pp. 1557–1565, Jun. 2017.

[18] T. Shao, Y. Zhou, C. Zhang, W. Yang, Z. Niu, and C. Ren, "Surface modification of polymethyl-methacrylate using atmospheric pressure argon plasma jets to improve surface flashover performance in vacuum," *IEEE Trans. Dielectr. Electr. Insul.*, vol. 22, no. 3, pp. 1747–1754, Jun. 2015.

[19] S. Chen, S. Wang, Y. Wang, B. Guo, G. Li, Z. Chang, and G. J. Zhang, "Surface modification of epoxy resin using He/CF_4, atmospheric pressure plasma jet for flashover withstanding characteristics improvement in vacuum," *Appl. Surf. Sci.*, vol. 414, no. 1, pp. 107–113, Aug. 2017.

[20] S. Yu, S. Li, S. Wang, Y. Huang, M. T. Nazir, and B. T. Phung, "Surface flashover properties of epoxy based nanocomposites containing functionalized nano-TiO_2," *IEEE Trans. Dielectr. Electr. Insul.*, vol. 25, no. 4, pp. 1567–1576, Aug. 2018.

[21] Y. Huang, D. Min, D. Xie, X. Wang, and S. Lin, "Surface flashover performance of epoxy resin microcomposites influenced by ozone treatment," in *Proc. IEEE-ISEIM*, Toyohashi, Japen, Sep. 2017, pp. 235–238.

[22] Y. Xing, Y. Shen, X. Song, Y. Yu, and M. Xiao, "Effects of electron beam irradiation on insulation characteristics of epoxy/AlN nanocomposites," *IEEE Trans. Appl. Supercond.*, vol. 29, no. 2, Jan. 2019, Art. no. 7700804.

[23] Y. H. Cheng, Z. B. Wang, and K. Wu, "Pulsed vacuum surface flashover characteristics of nano-micro composites," *IEEE Trans. Plasma Sci.*, vol. 40, no. 1, pp. 68–77, Jan. 2012.

[24] Z. Zhang, X. Zheng, Y. Jin, J. Wu, W. Wu, and W. Lei, "Surface flashover characteristics in polyimide/ZnO nanocomposite under DC voltage in vacuum," *IEEE Trans. Dielectr. Electr. Insul.*, vol. 22, no. 5, pp. 2951–2957, Nov. 2015.

[25] D. Min, W. Wang, and S. Li, "Numerical analysis of space charge accumulation and conduction properties in LDPE nanodielectrics," *IEEE Trans. Dielectr. Electr. Insul.*, vol. 22, no. 3, pp. 1483–1491, Jun. 2015.

[26] D. Min, S. Li, and Y. Ohki, "Numerical simulation on molecular displacement and DC breakdown of LDPE," *IEEE Trans. Dielectr. Electr. Insul.*, vol. 23, no. 1, pp. 507–516, Mar. 2016.

[27] S. Li, G. Yin, S. Bai, and J. Li, "A new potential barrier model in epoxy resin nanodielectrics," *IEEE Trans. Dielectr. Electr. Insul.*, vol. 18, no. 5, pp. 1535–1543, Oct. 2011.

[28] S. Li, G. Yin, G. Chen, J. Li, S. Bai, L. Zhong, Y. Zhang, and Q. Lei, "Short-term breakdown and long-term failure in nanodielectrics: A review," *IEEE Trans. Dielectr. Electr. Insul.*, vol. 17, no. 5, pp. 1523–1535, Oct. 2010.

[29] N. Longiéras, M. Sebban, P. Palmas, A. Rivaton, and J. L. Gardette, "Degradation of epoxy resins under high energy electron beam irradiation: Radio-oxidation," *Polym. Degradation Stability*, vol. 92, no. 12, pp. 2190–2197, 2007.

[30] G. Smets, G. Weinand, and S. Deguch, "Radical block polymerization of vinyl chloride. I. Ozonized polypropylene oligomers as heterofunctional initiator," *J. Polym. Sci. A, Polym. Chem.*, vol. 16, no. 12, pp. 3077–3090, Dec. 1978.

[31] G. Blaise, "New approach to flashover in dielectrics based on a polarization energy relaxation mechanism," *IEEE Trans. Electr. Insul.*, vol. 28, no. 4, pp. 437–443, Aug. 1993.

[32] G. Blaise and C. Le Gressus, "Charging and flashover induced by surface polarization relaxation process," *J. Appl. Phys.*, vol. 69, no. 9, pp. 6334–6339, 1991.

[33] D. M. Min and S. T. Li, "Simulation on the influence of bipolar charge injection and trapping on surface potential decay of polyethylene," *IEEE Trans. Dielectr. Electr. Insul.*, vol. 21, no. 4, pp. 1627–1636, Aug. 2014.

[34] S. Li, D. Min, W. Wang, and G. Chen, "Modelling of dielectric breakdown through charge dynamics for polymer nanocomposites," *IEEE Trans. Dielectr. Electr. Insul.*, vol. 23, no. 6, pp. 3476–3485, Dec. 2016.

[35] J. Y. Li, F. S. Zhou, D. M. Min, S. T. Li, and R. Xia, "The energy distribution of trapped charges in polymers based on isothermal surface potential decay model," *IEEE Trans. Dielectr. Electr. Insul.*, vol. 22, no. 3, pp. 1723–1732, Jun. 2015.

[36] T. Mizutani and M. Ieda, "Carrier transport in high-density polyethylene," *J. Phys. D, Appl. Phys.*, vol. 12, no. 1, pp. 291–296, Jul. 1979.

[37] Z. Zhang, X. Qiao, Y. Zhang, L. Tian, D. Zhang, and X. Liang, "AC flashover performance of different shed configurations of compositeinsulators under fan-shaped non-uniform pollution," *High Voltage*, vol. 3., no. 3, pp. 199–206, Sep. 2018.

[38] Z. Zhang, J. Zhao, D. Zhang, X. Jiang, Y. Li, B. Wu, and J. Wu, "Study on the dc flashover performance of standard suspension insulator with ring-shaped non-uniform pollution," *High Voltage*, vol. 3, no. 2, pp. 133–139, Jun. 2018.

[39] C. Y. Li, C. Lin, B. Zhang, Q. Li, W. Liu, J. Hu, and J. He, "Understanding surface charge accumulation and surface flashover on spacers in compressed gas insulation," *IEEE Trans. Dielectr. Electr. Insul.*, vol. 25, no. 4, pp. 1152–1166, Aug. 2018.

SHENGTAO LI (M'96–SM'11) received the Ph.D. degree in electrical engineering from Xi'an Jiaotong University (XJTU), China, in 1990. He was a Lecturer, an Associate Professor, and a Professor of XJTU, in 1990, 1993, and 1998, respectively. He was a Research Fellow at Waseda University, Japan, in 1996, and was also a Senior Visiting Scholar at the University of Southampton, U.K., in 2001. From 1993 to 2003, he was the Deputy Director of the State Key Laboratory of Electrical Insulating and Power Equipment (SKLEIPE), XJTU, where he has been an Executive Deputy Director, since 2003. His research interests include dielectrics and their application, insulating materials, and electrical insulation. He was awarded a Distinguished Young Scholar of China by the National Science Foundation, in 2006. He gave Liu Ziyu Memorial Lecture on the 11th International Conference on the Properties and Applications of Dielectric Materials (ICPADM), in 2015. He was the Chair of the 6th International Conference on Conditional Monitoring and Diagnosis (CMD), in 2016, and the 1st International Conference on Electrical Materials and Power Equipment (ICEMPE), in 2017. He is an Associate Editor of the IEEE TRANSACTIONS ON DIELECTRICS AND ELECTRICAL INSULATION.

ZHEN LI was born in Xi'an, China, in 1992. He received the B.S. degree in electrical engineering from Xi'an Jiaotong University, where he is currently pursuing the Ph.D. degree in high voltage and engineering technique. His main research fields are surface flashover and short-term breakdown characteristics of nanocomposites.

YIN HUANG was born in Shandong, China. He received the B.Sc. degree in electrical engineering from Xi'an Jiaotong University, in 2010, where he is currently pursuing the Ph.D. degree in high voltage and insulation technology with the State Key Laboratory of Electrical Insulation and Power Equipment. His research interests include polymeric insulating materials and surface flashover of the materials.

HAOMING XU received the B.S. degree in electrical engineering from Beijing Jiaotong University. He is currently pursuing the degree in high voltage and engineering technique with Xi'an Jiaotong University. His main research interest includes the surface flashover of nanocomposites.

FAROOQ ASLAM was born in Pakistan, in 1986. He received the B.S. degree in electrical engineering from the University of Engineering and Technology, Peshawar. He is currently pursuing the Ph.D. degree with the State Key Laboratory, School of Electrical Engineering, Xi'an Jiaotong University, China. His main researches focus on surface flashover and short-term breakdown characteristics of nanocomposites.

DAOMIN MIN received the Ph.D. degree in electrical engineering from Xi'an Jiaotong University (XJTU), China, in 2013. He was a Ph.D. Visiting Student with the Laboratory of Spacecraft Environment Interaction Engineering, Kyushu Institute of Technology, Japan, from 2010 to 2011, under the support of China Scholarship Council. Since 2013, he has been a Lecture with XJTU. From 2014 to 2015, he was a Junior Researcher at the Research Institute for Materials Science and Technology, Waseda University, Japan. His main research is charge transport and electrical breakdown properties of polymeric insulating materials.

WEIWANG WANG was born in Shaanxi, China, in 1987. He received the B.Sc. degree in electrical engineering from the Harbin University of Science and Technology, in 2010, and the Ph.D. degree from the School of Electrical Engineering, Xi'an Jiaotong University (XJTU), in 2015. Since 2016, he has been a Lecturer of XJTU. He is currently a Postdoctoral Fellow with the Measurement and Electric Machine Control Laboratory, Department of Mechanical System Engineering, Tokyo City University, Japan. His research interests include dielectric materials and space charge measurement.